Effect of Fibre Reinforcement on Mobilized Shear Strength of a Residual Soil at an Imposed Plane

A. H. Adegoke[1], and F. N. Okonta[2]

[1]Civil Engineering Science Department, University of Johannesburg, Auckland Park Kingsway Campus, P.O. Box 524, Auckland Park, 2006, South Africa, habeebadesola1@gmail.com
[2]Civil Engineering Science Department, University of Johannesburg, Auckland Park Kingsway Campus, P.O. Box 524, Auckland Park, 2006, South Africa, fnokonta@uj.ac.za

Abstract

The application of geosynthetic materials in soil engineering has shown improvement in soil mechanical properties and benefits to landfills liners, slope embankments, and many other applications have been documented. Discrete and strand fibres from synthetic and natural materials have also been used in geotechnical applications, and documented literature has reported significant improvement on the strength of primarily medium soils and tensile properties, especially improvement in ductility and residual strength. It is also reported that randomly distributed discrete and strand fibres interfere with preferred failure planes and modifies the anisotropic stress state of compacted soils. In embankment and soil engineering applications that rely on compaction, layer by layer compactions can impose potential failure planes in the embankments that can affect the stability of the formation. For such compactions, the use of randomly distributed fibres can improve the stability of the formation. A laboratory direct shear study was proposed to evaluate the effect of discrete sisal fibres on mobilized shear strength parameters in soil with compaction-induced planes. Series of direct shear stress were conducted on residual soils in which different planes (0, 15°, 30°, and 45°) were induced by compaction. Residual soil with and without sisal fibres was compacted and investigated. The mobilized shear strength parameters, including ductility and residual strengths, were evaluated. The results provide a preliminary indication of field compaction protocol and stability of fibre reinforced embankment.

Keywords: *Sisal fibre, direct shear parameters, compaction induced planes, embankment stability*
.

1 Introduction

Many slopes in Africa and tropical regions are subjected to varying climatic conditions. Such conditions render the slopes unable to withstand the required design loads and make them susceptible to high settlements with associated excessive distress, leading to a loss in slope stability. Many slopes stability studies have indicated that the infiltration of water into the slope decreases the stability of the slope (Gasmo et al., 1999; Liu et al., 2017; and Latief and Zainal, 2019). The overall stability of a geostructural system and the integrity of the geosynthetics are both dependent on the shear strength at the interface between the various materials. Many natural and artificial factors lead to slope failure and instability. Some of the natural ways the slope fails are the soil materials on which the slope is to be constructed (i.e., the founding conditions), the environmental conditions, the location of the groundwater table, and the stress history of the soil. One of the significant artificial factors contributing to the failure of a slope is the angle at which the slope is compacted. The potential causes for slope instability range from deep-seated failure (landslide) to surface erosion by wind or water (Kumar and Das, 2017). Road embankments are constructed on soft soil foundations or in areas where sinkholes or voids exist underneath the embankment, and they face the threat of excessive settlement or different settlement (Lu et al., 2020). Relatively broad exposure to the evaluation of the shearing resistance between various geosynthetic and soils has been presented in the technical literature.

Applications of soil strengthening, or stabilization range from mitigating complex slope hazards and increasing the subgrade stability (Pradhan et al., 2011). The stabilization of slopes in constructional project work is always critical as there is every possibility that the structures might collapse if the slopes are unstable. Several methods have been utilized to improve slopes' stability, which is adopted either singly or combined. It is well stated that the choice of stabilization depends on the costs and the consequences of such failure (Shukla, 2017). Several years back, different methods have been developed for soil stabilization and ground improvement in general (Pradhan et al., 2011). Broms and Wong (1990) classified the various forms of slopes stabilization as geometric methods by which the geometry of the slope is changed, hydrological processes at which the water content of the soil is reduced, and chemical and mechanical methods at which the sliding soil mass is increased or the external force causing the slope failure is reduced. Fiber-reinforced soil is a soil mass that contains randomly distributed, discrete elements (fibres). It has been recorded in kinds of literature by different researchers that fiber improves the mechanical behavior of the soil. The tensile resistance in fibres is mobilized by the normal stresses that act on the soil composite, imparting greater shear strength to the soil. Most importantly, the behavior of plant roots is replicated

using random discrete flexible fibres, which adds strength to the soil mass and contributes to its stability (Ramkrishnan et al., 2019).

Discrete randomly distributed fibers are typically applied to improve the soil's engineering characteristics, and consequently, the soil properties such as shear strength, density, compressibility, and hydraulic conductivity (Fard et al., 2021). Soil strength can be assessed from either laboratory or field tests, but different strengths are measured in the different tests. These differences are attributable to different stress conditions imposed in different tests (Atkinson and Lau, 1991). To compare soil strengths in different tests, it is important to ensure that the soil is brought to identical failure states. So, it is necessary to define the reference strength carefully. In typical laboratory tests, soil samples will reach different peak strengths and ultimate, critical states, and strengths. After very severe distortion, they may also reach residual states. It has been reported that during a simple shear test, the principal axes of stress and strain rotate, and the conditions within the test specimen are believed to represent those in the field in and around a developing rupture zone. Skempton, 1964 stated that at the critical state, the soil would continue to shear at a constant state so that all effective stresses and the volume remain constant, and at this critical state, grains may be rotating, so the shearing is turbulent; this distinguishes the critical state from the residual state when clay grains slip without rotation, so the shearing is laminar. It has been seen from the literature that different methods and laboratory tests have been conducted to simulate and compare the results of a triaxial test with that of a simple shear test. The specimen size, preparation method, load controlling feedback for triaxial, and simple shear are often different, introducing some uncertainties in a direct comparison of experimental data (Rahman and Nguyen, 2021).

However, based on the premise that many slope failures occurred at an angle at which they are compacted during layer-by-layer compaction, this mode of failure is not well observed. Still, it is a significant concern for civil engineers and the entire populace. For the reasons mentioned above, there is a need to thoroughly investigate the effects of stranded fibres on the geometry of the plane of failure of compacted slopes at different angles. Also, since the stress conditions in a simple shear test are like those in a conventional direct shear test (Atkinson and Lau, 1991), but comparison or relation between these conditions is minimal due to the lack of studies for critical state behavior in direct shear. Therefore, there is a need to investigate the critical stress of an embedded plane in a direct shear test to mimic that of conventional simple shear. Thus, the authors are motivated to study the mobilized shear strength parameters, including ductility, residual strengths, critical stress, to provide a preliminary indication of field compaction protocol, mimic the simple shear test, and the stability of fibre reinforced embankment. This study will enable the slopes to last longer and modify the plane of failure and contribute to existing knowledge.

2 Materials and Methods

2.1 Materials

The residual soil sample used herein was locally collected and sourced from a construction site within Johannesburg, South Africa. The soil lumps were broken into small pieces and screened through a 4.36 mm size sieve to free them from roots, pebbles, gravel, etc. The soil was screened to have a homogeneous mass containing sand to clay. During this research, commercially available sisal fibre was used for the soil reinforcement. A South African company supplied commercially available sisal fibres used in this study. The fibres were provided in a specified length (12 mm).

2.1.2 Properties of Soil

The soil used in the investigation was classified as well-graded sand with clay (SW-SC) according to Unified Soil Classification System and well-graded sand with clay A-2-5 (0) AASHTO Soil Classification System. The liquid and plastic limits of the soil were found to be 41.54 % and 34.44 %, respectively. The mean grain sizes (D_{10}, D_{30}, and D_{60}) are 0.145 mm, 0.525 mm, and 0.1781 mm. The soil was composed of 10.13 % gravel, 83.49 % sand, 3.09 % silt, and 3.29 % clay (6.38% fines). The soil had a maximum dry density of 1671 kg/m^3 with optimum moisture content (OMC) of 18.01 %, and a specific gravity of 2.85. Table 1 below highlighted the properties of the soil.

Table 1. Soil properties

USCS Soil Classification	well-graded sand with clay (SW-SC)
AASHTO Soil Classification	well-graded sand with clay A-2-5 (0)
Mean grain size D10 (mm)	0.145
Mean grain size D30 (mm)	0.525
Mean grain size D60 (mm)	0.1781
Cu	12.28
Cc	1.07
Gravel % (> 4.75 mm)	10.13
Sand % (4.75-0.75 mm)	83.49
Fines % (< 0.075 mm)	6.38
Silts % (0.075-0.002 mm)	3.09
Clay % (< 0.002 mm)	3.29
Liquid Limit (%)	41.54
Plastic Limit (%)	34.44
Plasticity Index (%)	7.10

Specific Gravity	2.85
MDD (kg/m^3)	1,671

2.1.3 Properties of Reinforcement

In this current research, the sisal fibre was used as reinforcement. The diameter (d) of the fibres used was 0.2 mm. The fibre was supplied in 12 mm form. Thus, the aspect ratio of the fiber used was 60. Single fibre tensile tests were conducted to determine fibre mechanical properties (Kafodya and Okonta, 2019). The summary of the results is shown in Table 2.

Table 2. Properties of the sisal fibre used in this study (Kafodya and Okonta, 2019)

Fibre property	Value
Breaking tensile strength (MPa)	500
Young Modulus (GPa)	23
Elongation at break (%)	2.1
Average diameter (mm)	0.2

2.2 Test Methods

In the present investigation, an attempt was made to study the effects of the inclusion of sisal fibers (with aspect ratio, l/d = 60) along the imposed plane on mobilized shear strength of locally available residual soil compacted to standard Proctor's maximum density. To determine the alteration in the slope failure of a preferred plane due to inclusion of fibers, and to mimic the critical states of soils in simple shear with an imposed planes using a direct shear test, a series of direct shear tests were conducted with un-reinforced as well as reinforced soil at four different normal stresses 50, 100, 150, and 200 kPa for different slopes at an angle of 0, 15, 30, and 45 degrees. For reinforced slopes, the fibre content was 0.75 %, reported to be the maximum fibre content for a given fibre-reinforced soil. Thus, series of direct shear tests were conducted at an imposed plane.

2.2.1 Sample Preparation

A square pipe of 100 mm x 100 mm was cut into four different angles (0, 15, 30, and 45 degrees) using a lathe machine with four molds for each angle to simulate a small scale of field compacted slope. Each mold was cut at about 50 mm long, with plane angle inclusive, and this was done to replicate the shear box used, 100 x 100 x 35 mm in size. Next, the rust at the innermost part of the molds and the rough edges were removed using sharp paper and files, respectively. Finally, a platform was prepared using a table and a set square to be manipulated to give the angle needed before commencing soil compaction inside the mold.

The molds and the platform were greased to avoid the difficulty of removing the samples after compaction. The fibre content used in this research is 0.75 % of the soil's total weight to avoid creating large voids within the compacted soils. The mass of the soil used was calculated from the relationship between the maximum dry density and the volume of the mold (volume of a triangular prism with a base angle). Soil samples were prepared by initial dry mixing of the residual soil and corresponding quantity of fiber (according to a percentage by weight of the soil). Then optimum water obtained from the standard proctor compaction test was added and remixed until the water spreads all over the soil. The dry and wet mixing of soil–fiber–water was carried out in a non-porous metal tray to avoid water loss. The soil, fibre, and water were mixed manually, spending sufficient time with proper care to get a homogeneous mix. The soil fibre composite was then placed in the prepared mold on the platform created before the initiation of compaction. Finally, the soil composite was compacted by tamping to standard Proctor's maximum density to obtain the specimens for direct shear tests. Figure 1 shows the vertical section of compacted induced plane samples after being removed from the mold at different angles (0, 15, 30, and 45 degrees, respectively) to simulate the embedded plane. The white line placed on the induced samples shows the parts that need to be trimmed to length (100 x 100 x 35 mm). The white line was made by rolling tissue paper into a desirable size and length for proper measurement. Following the preparation, samples were consolidated for five minutes inside the shear box before shearing.

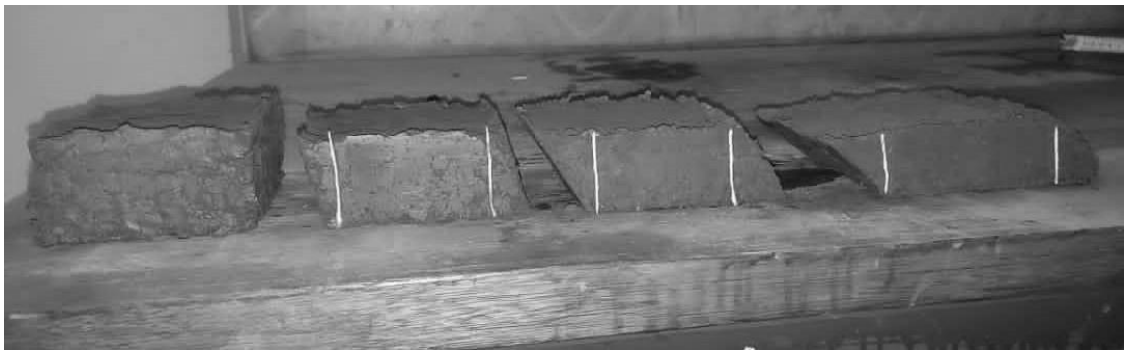

Figure 1. Vertical section of an embedded plane samples

2.3 Residual Soil Shear Strength Measurement

The experimental study involved performing a series of direct shear tests in a 100 mm x 100 mm shear box in a plane and 35 mm in depth. The tests were carried out with constant normal effective stresses only. Constant normal stresses were applied by dead weights acting through a lever. Normal and shearing loads were measured using proving rings, and dial gauges measured vertical and horizontal displacement. All the samples were soaked for about five minutes in the shear box before the commencement of the test. Tests were carried out on each interface at applied normal stresses of 50, 100, 150, and 200 kPa with virgin samples used for each of the normal stresses compacted at different angles; 0, 15, 30, and 45 degrees. A shearing rate of 0.3 mm/min was used for all tests under normal stresses of 50, 100, 150, and 200 kPa, and the samples were sheared against the angles. The displacements and the corresponding shear forces were recorded at specified time intervals when the samples underwent a shear displacement up to 10 mm or failure. Once the maximum displacement or failure was achieved, the box was unclamped, and the soil was carefully removed from the box. Once the sample was released, the box was cleaned with water and wiped with clothes for the next test.

According to the Mohr-Coulomb theory, the displacement versus the shear force was plotted on the graph for the envelope. The slope of the best-fit line corresponded to the total friction angle, while the intercept of the fitting line corresponds to the total cohesion. The Mohr-Coulomb theory is usually expressed as an equation to calculate the shear strength of saturated soils (Hongde et al., 2021).

3.0 Results and Discussion

Several tests were conducted on soil without reinforcement (sisal fibre) and randomly distributed discrete fibre-reinforcement (0.75 % by weight of air-dry soil) at an aspect ratio l/d = 60. The effect of fiber inclusion on stress-displacement behavior and shear stress parameters concerning modifying the preferred plane of failure, ductility, and the critical stress path are discussed below.

3.1 Shear Stress Displacement Response

The stress-displacement of soils reinforced with fibre content and length (0.75 % and 12 mm, respectively) and unreinforced samples for an embedded plane obtained from direct shear tests are presented in Figure 2 and Figure 3, respectively. Figure 2 shows the data as the shear stress against the horizontal displacement. It can be inferred from the figures that the samples under constant stresses reached their critical state reasonably well at 6 mm horizontal displacement and become residual when the shear strain is in excess. This critical state is more pronounced for the embedded plan, and this shows a typical representation of soil compacted and shared in a simple shear box. Also, a compacter compacting a slope at an angle more than 15 degrees tends to be thrown away during compaction at this critical state.

It can be observed in Figure 2, and Figure 3 that the maximum shear strength of the unreinforced samples was observed at about 6 mm horizontal displacement compare with that of reinforced samples in which the shear strength keeps increasing beyond the completion of the tests. The rapid reduction in shear strength of the unreinforced samples compared with the relative increase in the reinforced samples shows how fibre improves the brittleness of the soil to a more ductile one. This trend suggests that; adding fibres to a soil medium that exhibits brittle material properties results in greater fiber connection and replacement of a portion of soil by an elastic material. As a result, the soil becomes softer, the elasticity of the medium increases, and as a result, the specimens fail at higher axial strains.

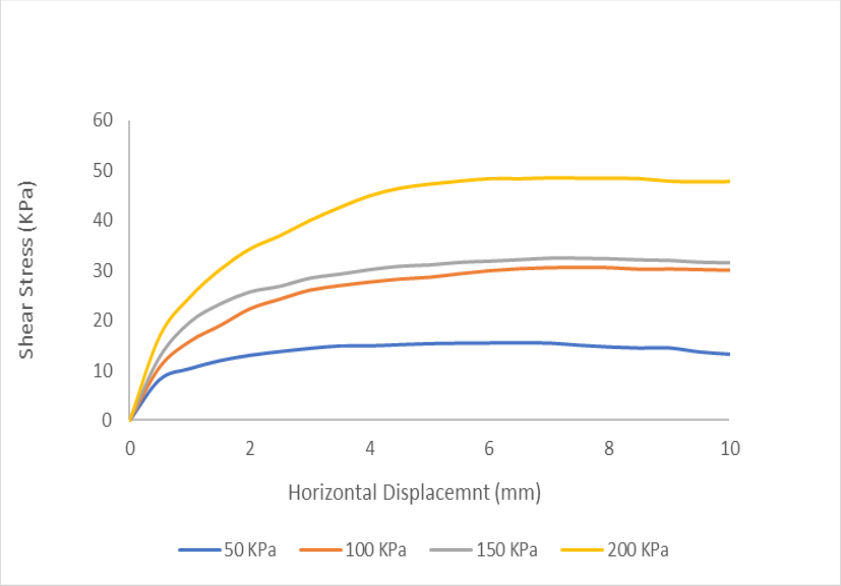

a

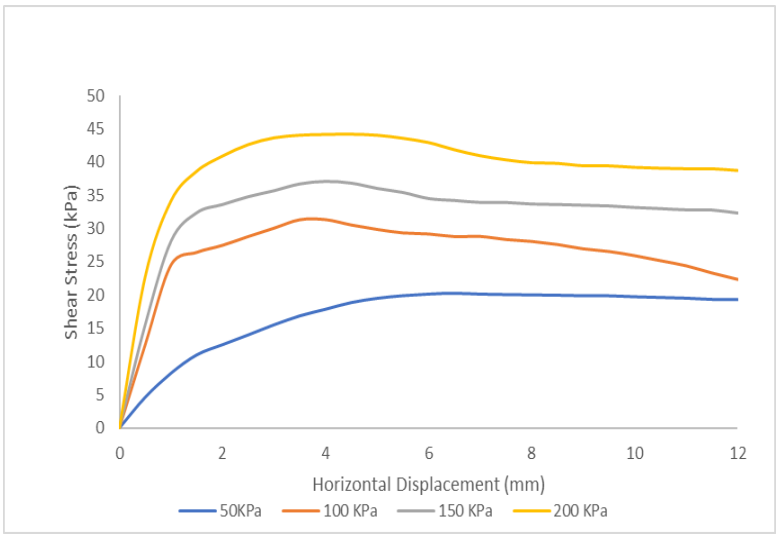

b

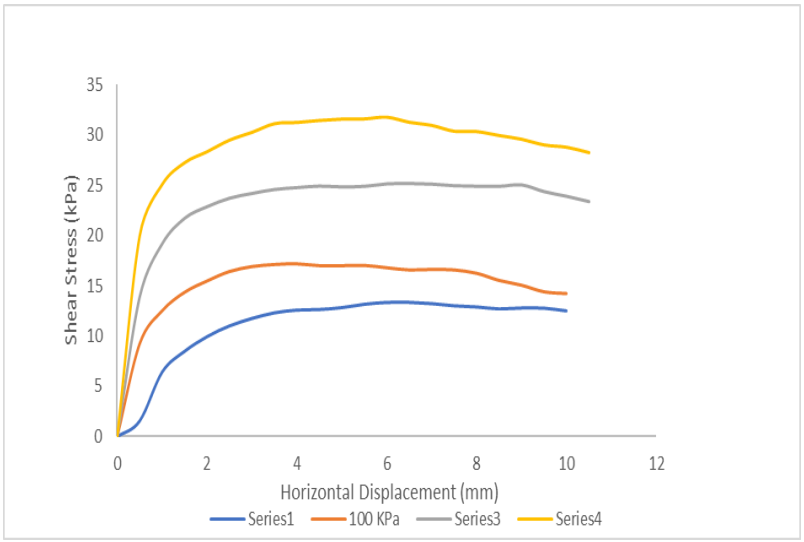

c

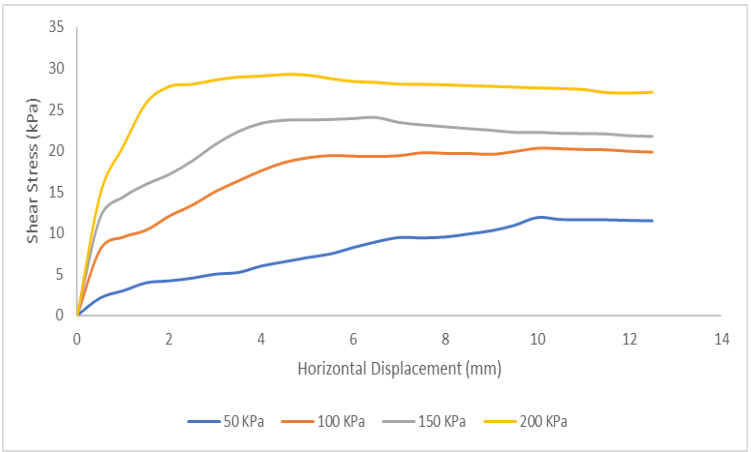

d

Figure 2. (a) shear stress displacement curve for unreinforced samples at 0 degrees, (b) shear stress displacement curve for unreinforced samples at 15 degrees, (c) shear stress displacement curve for unreinforced samples at 30 degrees, and (d) shear stress displacement curve for unreinforced samples at 45 degrees

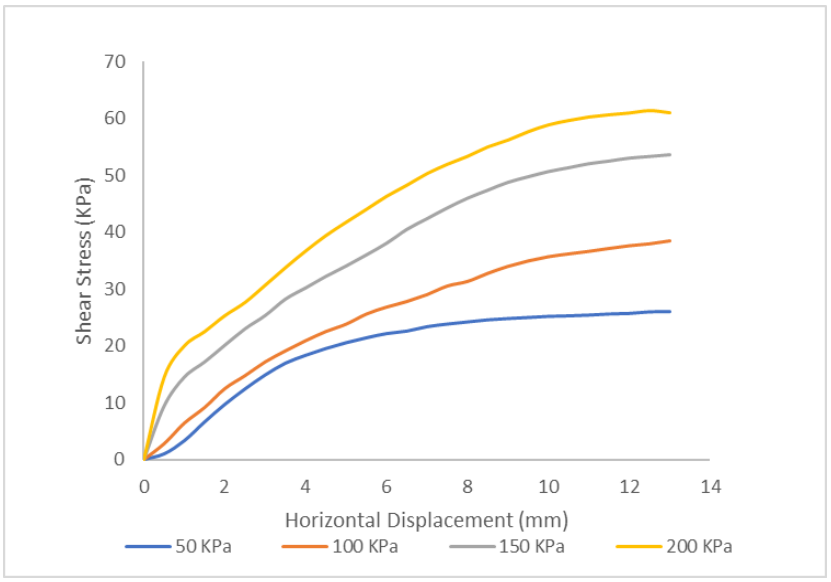
Shear Stress (KPa)
70
60
50
40
30
20
10
0
0
2
4
6
8
10
12
14
Horizontal Displacement (mm)
50 KPa
100 KPa
150 KPa
200 KPa

a

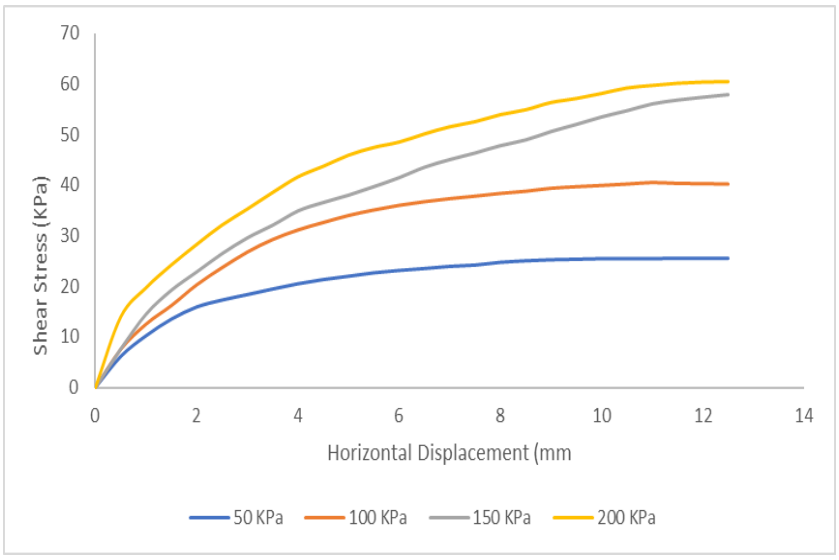
Shear Stress (KPa)
70
60
50
40
30
20
10
0
0
2
4
6
8
10
12
14
Horizontal Displacement (mm
50 KPa
100 KPa
150 KPa
200 KPa

b

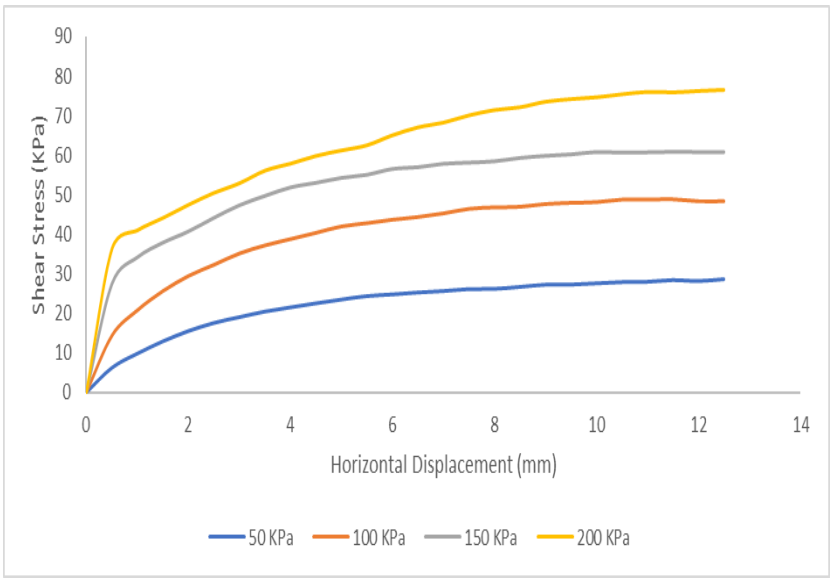
Shear Stress (KPa)
90
80
70
60
50
40
30
20
10
0
0
2
4
6
8
10
12
14
Horizontal Displacement (mm)
50 KPa
100 KPa
150 KPa
200 KPa

c

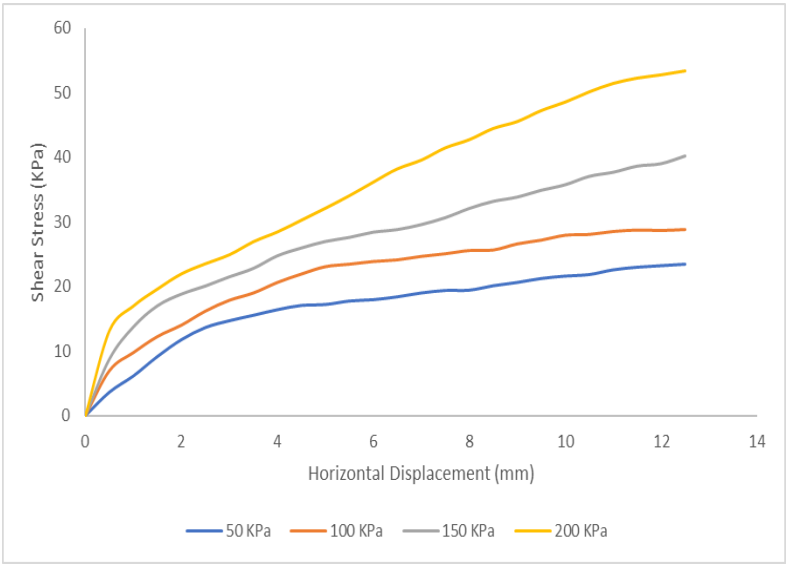

d

Figure 3. (a) shear stress displacement curve for reinforced samples at 0 degrees, (b) shear stress displacement curve for reinforced samples at 15 degrees, (c) shear stress displacement curve for reinforced samples at 30 degrees, and (d) shear stress displacement curve for reinforced samples at 45 degrees

3.2 Shear Strength Parameters

The direct shear test results were plotted in Mohr-Coulomb shear failure envelopes for unreinforced and fibre reinforced soils at different induced planes (Figure 4). The shear stress at failure is the ultimate shear strength produced during shearing of the soil and reflects the ability of the soil to resist shear sliding (Hongde et al., 2021). As shown in Figure 4, the shear stress at failure increased with increasing net normal stress and showed an approximately linear dependence, which the Mohr-Coulomb theory could support. The ultimate shear strength at four net normal stresses composes the shear failure envelope of the soil. Differences in the shear failure envelopes could be found between different samples at different induced planes for reinforced and unreinforced samples.

The observed shear parameters (c and φ) shown in Table 3 indicate that the reinforced soil exhibits an increase in the angle of internal friction (φ) and the cohesion (c) in comparison to the unreinforced soil for different imposed angle. The increase in the angle of internal friction of the reinforced samples shows how fibre modified the plane of failure of an embedded plane. The illustration of how fibre modified the induced plane is clearly shown in Figure 5 for 100 kPa normal stress. This modification in the induced plane occurs because fibre tends to optimize the friction angle for an embedded plane (that is, oppose the direction of failure) and not the cohesion. From Figure 4, it is clearly shown that all reinforced soils' failure envelope is slightly curved compared with the failure envelope of the unreinforced ones where the curve is more pronounced for the 0-degree embedded plane.

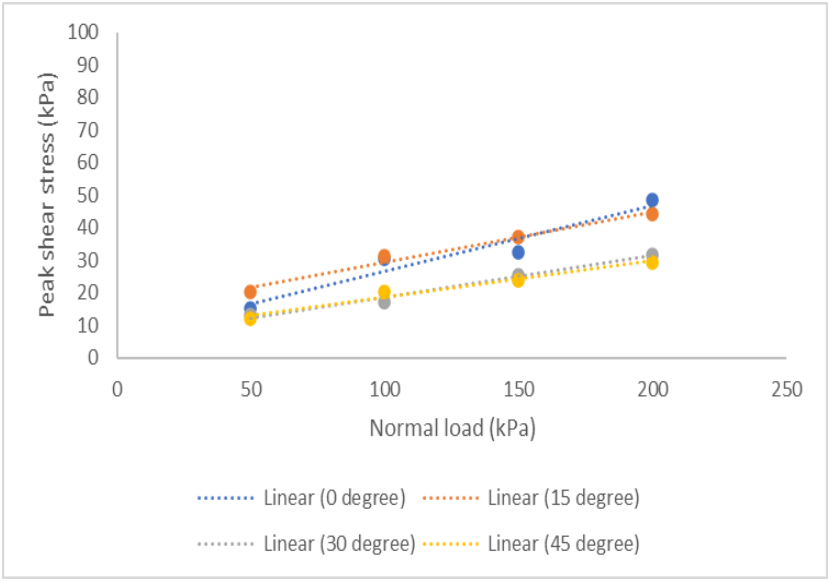

a

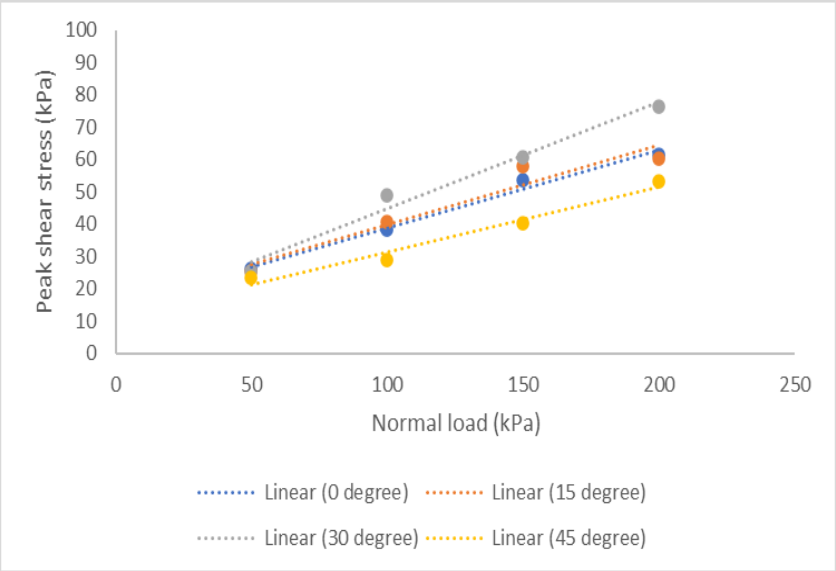

b

Figure 4. (a) Failure envelope curve for unreinforced samples for embedded planes and (b) failure envelope curve for reinforced samples for an embedded planes

Table 3. Failure envelope parameters for reinforced and unreinforced samples of an embedded planes

Unreinforced induced plane (º)	**Cohesion, C (kPa)**	**The angle of internal friction, φ (º)**	**Fiber-reinforced induced plane (º)**	**Cohesion, C (kPa)**	**The angle of internal friction, φ (º)**
0	6.4	11.44	0	14.57	13.63
15	13.93	8.77	15	15.51	13.76
30	6.05	7.22	30	14.78	17.29
45	7.38	6.39	45	11.08	11.48

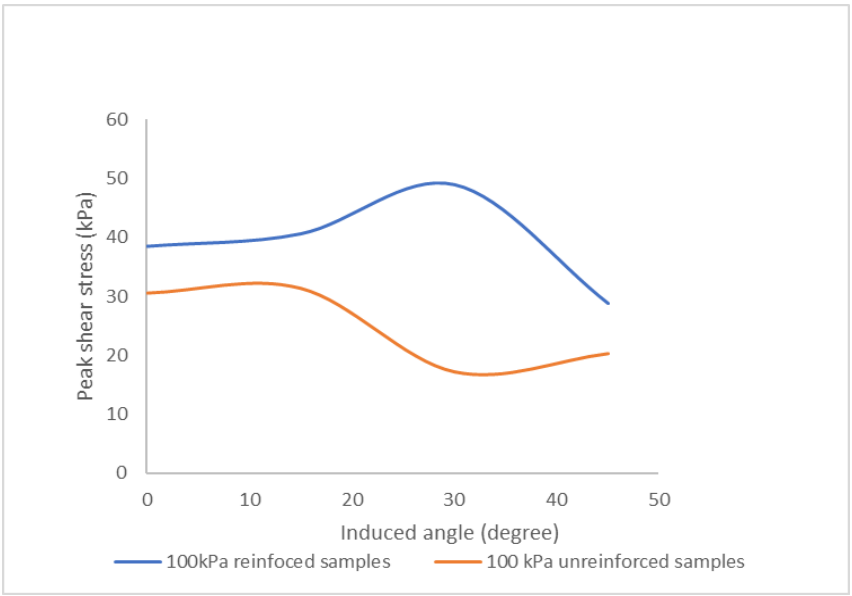

Figure 5. Peak shear strength versus induced angle for unreinforced and fibre reinforced samples at 100 kPa normal stress

4.0 Concluding remarks

The effect of fibre reinforcement on mobilized shear strength of a residual soil at an imposed plane under applied normal stresses has been investigated using the direct shear test. The strategy explicitly considers the homogeneous distribution of fibre within the soil matrix and the bedding plane of failure imparted on the soil samples. The results obtained from the embedded plane without fibre clearly showed that the direct shear test could mimic the simple shear if an induced plane of failure in the samples can be tested. In the case of an embedded plane, the shear strength of the embedded plane increases with the addition of sisal fibre compared with the embedded plane without fibre. Furthermore, the increment in the angle of internal friction of the embedded samples reinforced with fibre compared with the unreinforced ones indicates fiber's ability to optimize friction angle and thereby modified the preferred plane of failure. Also, the ductility of the fibre reinforced samples increased compared to the brittleness of the unreinforced samples. This shows how fibre can alter the anisotropic behavior of soils to more isotropic states.

The results presented in this paper show that the strategy can accurately alter the plane of failure of a slope concerning the angle at which it was compacted during construction and opens the possibility of using sisal fibre during layer-by-layer compaction of slope compacted at different angles considering the cost, mode of installation, time, and the long-term effects. Indeed, further validation of this technique is necessary to gain confidence and to assess its limitations. Nevertheless, one step in this direction has been achieved and presented in this paper: effect of fibre reinforcement on mobilized shear strength of a residual soil at an imposed plane whose experimental reproduction is highly complex and tactical in terms of getting the accurate bedding plane, the volume of soil fibre composite to fill the mold of different angles from the maximum dry density obtained from the proctor compaction and the analytical aspect of the parameters.

References

Atkinson J. H., and Lau W. H. W., 1991. Measurement of soil strength in simple shear tests. Canadian Geotechnical Journal 28: 255 - 262

Broms, B. B., and Wang, K. S., 1990. Landslide in foundation Engineering Handbook (ed. H. Y. Fang), Van Nostrand Reinhold, New York, USA.

Fard S. H., Konig, D., and Goudarzy, M., 2021. Plane strain shear strength of unsaturated fiber-reinforced fine- grained soils. Acta Geotechnical.

Gasmo, J. M., Rahardjo, H., and Leong, E. C., 2000. Infiltration effects on stability of a residual soil slope. Journal of Computers geotechnics 26(2): 145-165.

Hongde, W., et al. (2021). Analysis of unsaturated shear strength and slope stability considering soil desalinization in a reclamation area in China. Catena 196 (2021) 104949.

Kafodya I. and F. N. Okonta, 2019. Cyclic and post-cyclic shear behaviors of natural fibre reinforced soil. International Journal of Geotechnical Engineering.

Kumar N., and Das D., 2017. Nonwoven geotextiles from nettle and poly (lactic acid) fibers for slope stabilization using bioengineering approach. http://www.elsevier.com/open-access/userlicense/1.0/.

Latief, R. H., and Zainal, A. K. E., 2019. Effects of Water Table Level on Slope Stability and Construction Cost of Highway Embankment. Journal of Engineering 23(5), 1-12.

Liu, J., et al. (2017). Stability analysis of road embankment slope subjected to rainfall considering runoff-unsaturated seepage and unsaturated fluid–solid coupling. International Journal of Civil Engineering 15(6), 865-876.

Lu, W., et al. (2019). Evaluation of geomembrane effect based on mobilized shear stress due to localized sinking. Journal of Advances in Civil Engineering.

Pradhan P. K., Kar, K., R., and Naik, A., 2011. Effect of Random Inclusion of Polypropylene Fibers on Strength Characteristics of Cohesive Soil. Journal of Geotechnical Geology Engineering. 30, 15–25

Rahman M. M., and Nguyen H. B. K., (2021). A comparison of critical state behaviour between triaxial and simple shear conditions: A DEM study. Proceedings of the 20th International Conference on Soil Mechanics and Geotechnical Engineering, Sydney 2021.

Ramkrishnan et al., 2019. Effect of random inclusion of sisal fibres on strength behavior and slope stability of fine grained soils. Materials Today: Proceedings. 5 (2018), 25313–25322.

Shukla S. K., 2017. Department of Civil Engineering, Harcourt Butler Tecnological Institute, Kanpur, India

Skempton, A.W. 1964. Long term stability of clay slopes. Geotechnique, 14: 77-101.